

## THE EXPERIMENTAL STUDY ON VISCOELASTIC MATERIAL DAMPERS AND THE FORMULATION OF ANALYTICAL MODEL

Mitsuo ASANO<sup>1</sup>, Higashino MASAHIKO<sup>2</sup> And Masashi YAMAMOTO<sup>3</sup>

### SUMMARY

The mechanical properties of visco-elastic damper are examined and the mechanical model of the damper is developed in this report. The dependency on frequency, amplitude and temperature in the mechanical properties of visco-elastic material must be evaluated appropriately. However, the properties of visco-elastic materials are not studied comprehensively. The mechanical properties of four kinds of materials, which are currently produced, are studied based on dynamic loading experiment of full-scale dampers. The two mechanical models are constructed. One considered the dependency on the number of repeated cycle and amplitude, and another considered the dependency on frequency. By comparing with the experimental results, the constructed models agreed accurately. The earthquake response analyses of a building with the dampers are carried out. The responses were reduced in the analyses remarkably.

### INTRODUCTION

Visco-elastic damper ( VE damper hereafter ) has the characteristic of absorbing vibration energy from small amplitude to large amplitude vibration. Hence, it can improve the habitability of the building during wind excitation and secure the safety of the structure during earthquake with same device. However, the mechanical properties of VE material have the dependencies on frequency, amplitude and temperature. These characteristics should be evaluated appropriately in the mechanical model, but the construction of mechanical models for analysis of these properties is rather complex.

Various mechanical models that can evaluate these dependencies have been proposed in the previous studies. In these studies, the dependency on frequency has been the major interest and this property has been widely studied using multi-Maxwell element model[Soda and Takahashi,1997], fractional derivatives model [Kasai, Munshi, Lai and Maison,1993], fading memory model[Izumi, Xue, Tobita and Hanzawa,1990], and etc. Among these models, fractional derivatives model and fading memory model have simple mathematical expression, however, element composition with these models are relatively complex. The non-linearity and reaction force degradation are also major properties of VE material, but the mechanical models for these properties have not been intensively studied as frequency dependency, because of the complexity of damping mechanism.

In this report, the authors have conducted the dynamic loading experiment of full-scale dampers of four different materials and examined the characteristics of these dampers. The mechanical properties of these dampers were roughly divided into two groups. The first group showed the characteristics of non-linearity and reaction force degradation. The second group showed the dependency on frequency but did not show noticeable non-linearity and reaction force degradation.

The authors constructed the mechanical models for these characteristics. For the first group, reaction force degradation was modeled in the relationship with absorbed energy. Non-linearity was modeled using four-

<sup>1</sup> Structural Engineering Department, Nagoya Branch, Takenaka Corporation Email:mistuo.asano@takenaka.co.jp

<sup>2</sup> Research & Development Institute, Takenaka Corporation

<sup>3</sup> Research & Development Institute, Takenaka Corporation

element multi-Maxwell model with one non-linear dashpot. For the second group, the dependency on frequency was modeled by ARX model, which corresponds to five-element multi-Maxwell model. The mechanical models constructed by these methods were compared with the results of the experiment by earthquake wave excitation, and the accuracy of these models was studied. Also, the structural control efficiency was examined by earthquake response analysis of a building.

## DYNAMIC LOADING EXPERIMENT OF VE DAMPERS

### Outline of experiment

The most fundamental utilization of VE-dampers in the framing system is bracing, as shown in Fig.1. The construction of a damper is also shown in Fig.1. VE-material layer is placed between two rectangular steel pipes. Each rectangular steel pipe must be connected to different floor levels. With this configuration, the inter-story drift of the framing system will induce the relative displacement between two steel pipes, and the shear deformation in VE-material layer will be induced, and the damping effect will thus be obtained.

In order to examine the mechanical properties of this damper, dynamic loading experiments were carried out using the apparatus shown in Fig.2. The dampers for four different kinds of VE materials, which are currently available in the market, were provided. The outline of VE-dampers tested is shown in Table 1. The thickness of VE material layer was all 10mm, while the total area of each material was slightly different. The excitation conditions are shown in Table 2. Each sinusoidal excitation had ten cycles. Excitation cases for higher frequencies were limited to low levels, because of the force limitation, 30 ton, of the dynamic actuator. The experiments were carried out for two different ambient temperatures.

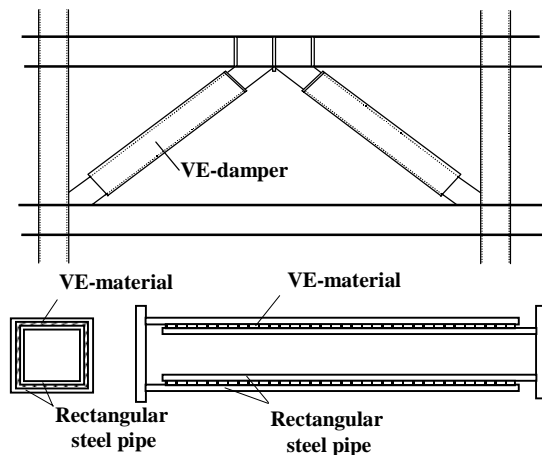


Figure 1: Configuration of VE-damper

Table 1: outline of VE-dampers tested

Title	VE-material compound	Shaer sequare	Ambient temperature	
			1	2
B1	Urethane-asphalt	8400cm <sup>2</sup>	23	12
B2	Rubber-Asphalt	7800cm <sup>2</sup>	25	10
B3	Acrylic	9000cm <sup>2</sup>	23	10
B4	Pine	9000cm <sup>2</sup>	28	10

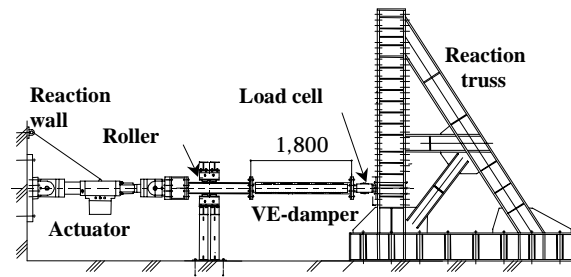


Figure 2: Testing apparatus

Table 2: Excitation conditions

Item	Excitation condition
Sinusoid	Frequency(Hz) B 2, 0.3, 0.5, 1.0, 2.0, 3.0
	Shear strain(%) B 10, 50, 100, 150, 200, 300
Sweep (only B3, B4)	Frequency(Hz) B 3 3.0
	Shear strain(%) B 0 Uniform
Earthquake response	Building B 4 layers first natural period B 0.05sec
	Input: El Centro 1940 NS Max: 50kine/j
	Maximum displacement B1: 1.0cm, B2: 1.5cm B3: 2.39cm, B4: 2.0cm

Sinusoidal excitation: 10 waves (Each case)

### Experimental results

The hystereses of four dampers are shown in Fig. 4. The diagrams in this figure are arranged in two series, different strain with constant frequency (0.2Hz), and different frequency with constant amplitude (shear strain:  $\gamma = 10\%$ ). These experiments were carried out in ambient temperature 1, shown in Table 1. B1 and B2 dampers showed oval shape hysteresis at shear strain level of 10% or less. But bi-linear shaped hystereses were observed at higher strain levels. Also the reaction force degradation was observed at large amplitude excitation, that large equivalent stiffness and loop area were decreased by the repetition of excitation. B3 and B4 dampers showed the oval hysteresis regardless of amplitude level. For these dampers, force degradation by the repetition of excitation was small.

Equivalent stiffness  $k_{eq}$  and equivalent damping  $h_{eq}$  of dampers subjected to sinusoidal excitation at temperature 1 are shown in Fig. 5 and Fig. 6 respectively. These values were evaluated by the rule shown in Fig.3. Second loop was used in the calculation for B1 and B2 dampers, since the reaction force degradation was observed in these

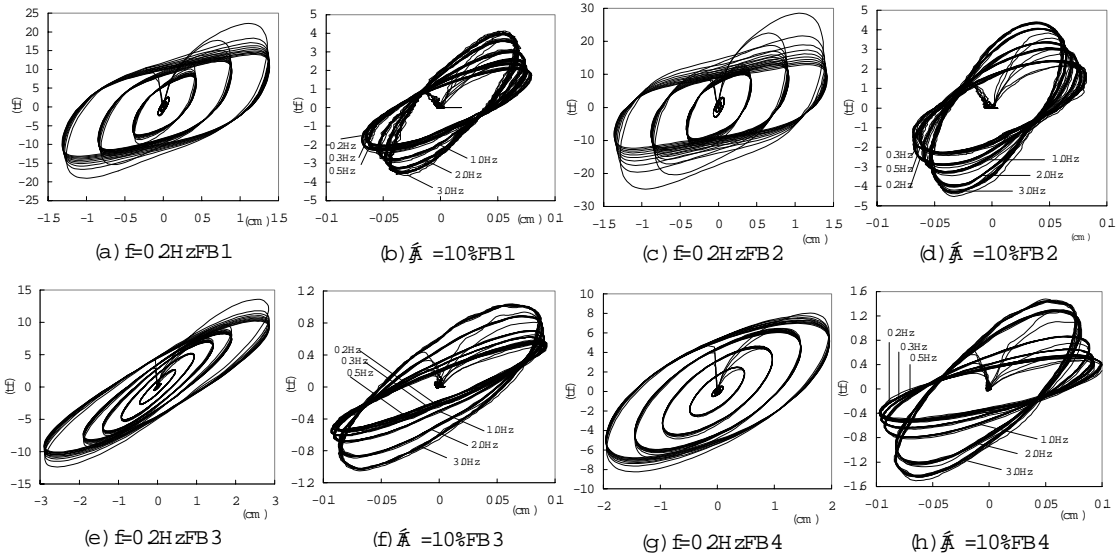


Figure 4 Hysteresis loop

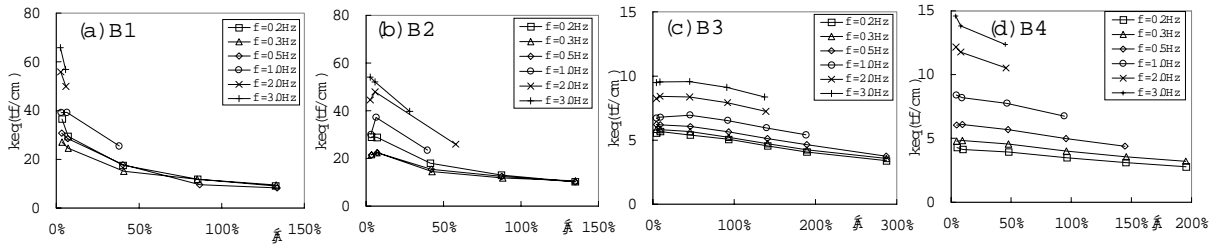


Figure 5 Equivalent stiffness

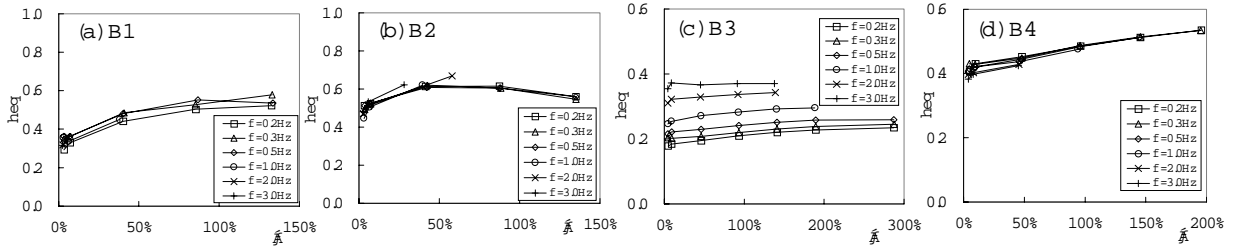


Figure 6 Equivalent damping

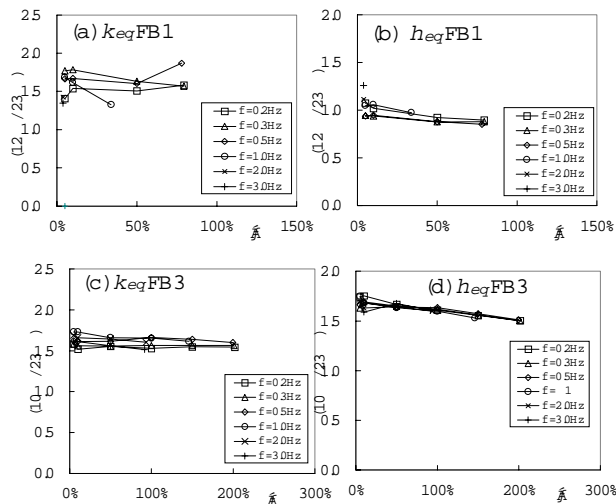
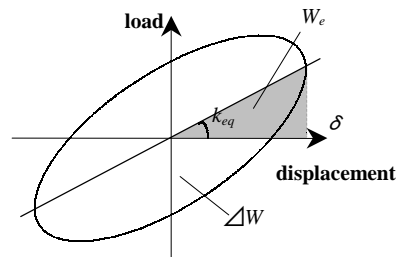


Figure 7 Temperature dependencies in equivalent stiffness and equivalent damping



$$W_e = \frac{1}{2} \cdot k_{eq} \cdot \delta^2$$

$\Delta W$ : hysteresis loop area

$$h_{eq} = \frac{1}{4 \cdot \pi} \cdot \frac{\Delta W}{W_e}$$

Figure 3 Calculation method of constants

dampers. The average value of all loops was adopted for B3 and B4 dampers, because the reaction force degradation was negligible for these dampers.

The dependency on frequency was observed in all four dampers, that equivalent stiffness increased as excitation frequency increased. This property was prominent in B3 and B4 dampers compared to B1 and B2 dampers. Also non-linearity was observed in all four dampers, that equivalent stiffness decreased as the excitation amplitude increased. However, this property in B3 and B4 dampers was not as noticeable compared to B1 and B2 dampers. Equivalent damping did not have any dependency on frequency for all dampers except B3. For B3 damper, equivalent damping increased as excitation frequency increased. The amplitude dependency in equivalent damping was relatively small for all dampers.

The value ratio at ambient temperature 1 to ambient temperature 2 for equivalent stiffness and equivalent damping are shown in Fig.7 for B1 and B3 dampers. For damper B1(12°C/23°C) , which represents the dampers have characteristics of non-linearity and reaction force degradation, the ratio in equivalent stiffness was almost 1.5 and the ratio in equivalent damping was almost 1.0. For damper B3(10°C/23°C) , which represents the dampers have dependency on frequency, ratio in both equivalent stiffness and equivalent damping was almost 1.6. Thus, both dampers, B1 and B3, showed dependency on ambient temperature.

## CONSTRUCTION OF THE MECHANICAL MODELS OF VE DAMPERS

The mechanical models of all four dampers are proposed after the experimental result shown in Chapter 2. In constructing the mechanical model, following assumptions were made:

- 1) Only ambient temperature 1 was considered.
- 2) Large earthquake was targeted.
- 3) Repetition number was relatively small.

### The modeling of VE dampers with reaction force degradation and non-linearity

The reaction force degradation and the non-linearity were modeled for B1 and B2 dampers. Fig.8 shows the relationship between the absorbed energy E and the reaction force degradation, when the sinusoidal excitations were imposed. The accumulated absorption energy E is expressed as follows:

$$E = \int_0^t F \cdot v dt \quad (1)$$

where, F is reaction force and v is the shear deformation velocity of VE material layer. The reaction force was normalized by the maximum force in this figure. Only the case for excitation frequency at 0.5Hz is shown in this figure, but similar results were obtained at other excitation frequencies. The results for amplitude 1.5cm and 1.0cm are shown in same figure. The reaction forces decreased by same rate to the amount of absorbed energy for different amplitude. It is commonly considered that the continuation time of the earthquake was shorter compared to the heat transmission rate, and all absorbed energy stayed inside the VE material layer. With this assumption, the all absorbed energy was evaluated as the rise of temperature of the VE material layer, in previous study. [Kasai, Huang and Wada,1997] However, the authors considered that, it is premature in the present material studies to think that only the rise of temperature caused the reaction force degradation. Thus, the amount of absorbed energy was directly chosen as the index. In Fig.8, reaction force degradation rate r is introduced, and the relationship between r and E can be expressed as follows:

$$r = 90 / (200 + 2E) + 0.55 \quad (2)$$

$$r = 150 / (200 + E) + 0.25 \quad (3)$$

Where, the expression (2) and (3) corresponds to damper B1 and B2 respectively. The expressions (2) and (3) are shown in bold lines in Fig.8. By transforming the original hysteresis with degradation rate r, the hysteresis, which was not influenced by degradation, was obtained as shown in Fig.9. Even the influence of degradation were removed, the hysteresis still have non-linearity. There are several methods to model the non-linearity, such as using bi-linear force-displacement relationship. [Yokokawa, Oishi and Soda, 1997] However, these models usually have relatively complex element composition. In this report, much simpler model using four- element model was introduced. This model contains only one non-linear element. The composition of four-element model is shown in the left figure of Fig.10.  $F_D$  represents the non-linear damping element, which has bi-linear force-velocity relationship shown in the right figure of Fig.10. This total model which is considering the reaction force degradation and non-linearity using four –element model will be referred as Degrading Bi-linear Velocity model (DBV model hereafter). By fitting the hysteresis with the corrected experimental results shown in Fig.9, each parameter for B1 and B2 dampers were identified as shown in Table 3. The fitted model is shown in Fig.11.



experimental results, the waves of reaction force in time domain appears to have good agreement. The ARX model simulated the experimental results very well for the hysteresis as well as the wave of reaction force in time domain. The results using Voigt model showed hysteresis with large area compared to experimental results, which indicates the overestimation of damping in this model.

**Table 3 Constants in DBV model**

Damper	B1	B2
$K_1$ (tf/cm)	7.0	15.0
$K_2$ (tf/cm)	25.0	120.0
$F_D$ (tf)	4.0	11.0
$C_1$ (tf $\cdot$ s/cm)	1.2	1.0
$C_2$ (tf $\cdot$ s/cm)	7.0	6.0
$C_3$ (tf $\cdot$ s/cm)	1.5	1.5

**Table 4 Constants in ARX model**

Damper	$a_1$	$b_1$	$b_2$	$b_3$
B3	-0.954	50.49	-89.85	39.58
B4	-0.961	62.33	-112.5	50.30

**Table 5 Constants in five-element multi-Maxwell model**

Damper	B3	B4
$K_1$ (tf/cm)	82.97	104.72
$K_2$ (tf/cm)	4.2	7.35
$K_3$ (tf/cm)	4.91	2.76
$C_1$ (tf $\cdot$ s/cm)	0.41	0.52
$C_2$ (tf $\cdot$ s/cm)	0.89	1.83

**Table 6 Constants in Voigt model**

Damper	Natural period(sec)	$k_{eq}$ (tf/cm)	$C$ (tf $\cdot$ s/cm)
B1	2.5	8.23	3.01
B2	2.5	10.2	4.55
B3	3.05	5.59	1.16
	2.5	5.86	1.11
B4	3.05	4.30	1.97
	2.5	4.84	1.84

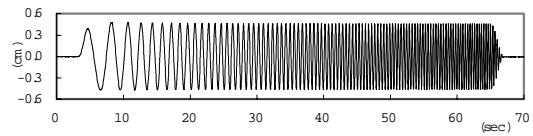


**Figure 12 Sweep wave (0.3~3.0Hz, shear strain:50%)**

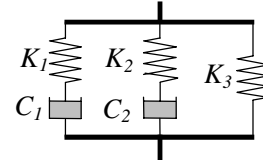


**Figure 13 Five-element multi-Maxwell model**

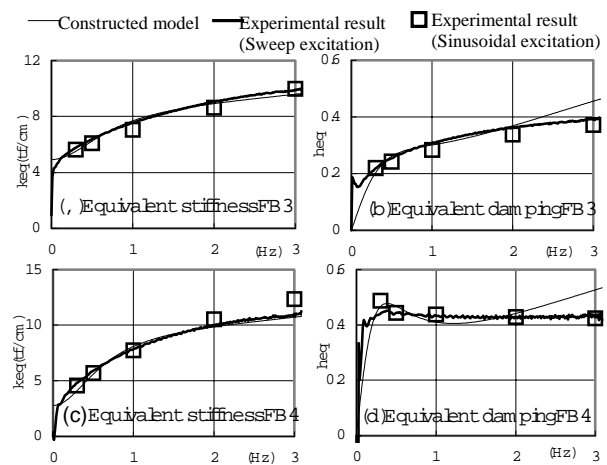


**Figure 14 Mechanical models and experimental results**

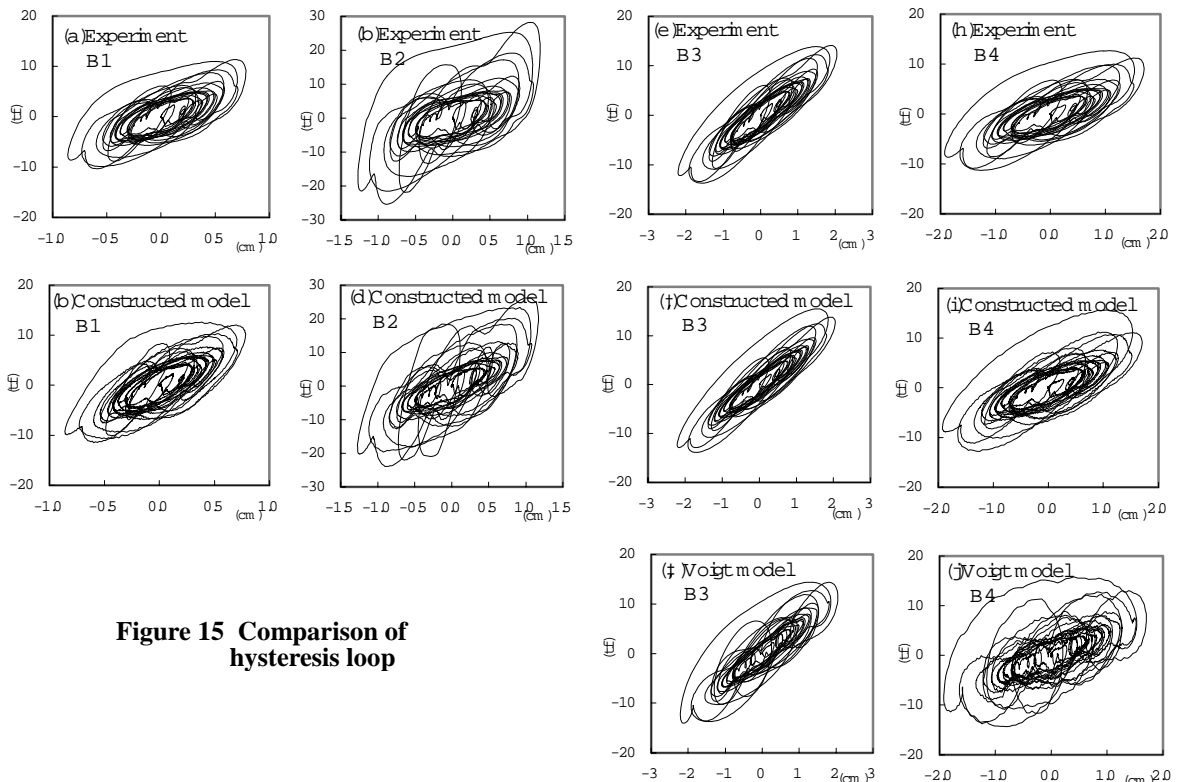


**Figure 15 Comparison of hysteresis loop**



